

Shape Optimization of Revolute Single Link Flexible Robotic Manipulator for Vibration Suppression

Sachindra Mahto

Abstract

In this work, shape optimization is carried out of a single link flexible revolute flexible manipulator. Robotic link is considered as an Euler-Bernoulli beam and finite element formulation is done for its dynamics analysis using Newmark's scheme. Sequential quadratic programming (SQP) method is used to minimize the dynamic maximum tip deflection in order to have vibration suppression. Optimized revolute robotic manipulator may be preferred in the real world applications as per vibration issue is concerned due to its flexible nature.

Keywords: Flexible revolute manipulator, Euler-Bernoulli beam, Shape optimization, Finite Element Method, Sequential quadratic programming

1 Introduction

Conventional robots are comprised of rigid links. For last few decades, flexible beams have been a topic of investigation in the field of robotics to replace some of the rigid links of the robot. Flexibility due to light weight has an importance due to several advantages (e.g. - require less material, higher manipulation speed, transport -able, etc.). However, there are some disadvantages associated with the flexible manipulators (e.g.-vibration problem due to low stiffness, etc.). Precision in positional accuracy and vibration control are the challenging tasks for researchers. Residual vibrations of flexible manipulators take time to settle down, which affects the subsequent operations of robotic tasks. This forcible delay needs optimal design of the robotic systems.

Most of the researchers optimized the fundamental frequency of the cantilever beam or manipulator. Cranch and Adler [1] presented the closed-form solutions in term of Bessel's functions for the natural frequencies and mode shapes of the unconstrained non-uniform beams with four kinds of rectangular cross-sections. Heidebrecht [2] determined the approximate natural frequencies and mode shapes of a non-uniform simply supported beam from frequency equation using Fourier sine series. Bailey [3] numerically solved the frequency equation derived from Hamilton's principle to obtain natural frequencies of the non-uniform cantilever beams.

Karihaloo and Niordson [4] determined the optimum tapering of a cantilever beam carrying an end mass to maximize fundamental frequency. Lio [5] developed a generalized method for the design of a cantilever beam of circular cross-section in flexural vibration. The beam is composed of two materials along the length. Wang [6] addressed optimum design of a single link manipulator to maximize its fundamental frequency. He formulated the design problem as a nonlinear eigenvalue problem using variational method. He demonstrated the increase of fundamental frequency as a result of optimization through numerical examples. Wang and Meirovitch [7] extended the work of Karihaloo and Niordson [4] to find substantial improvement in optimum shape through simplifying original analysis and solution procedure.

Sachindra Mahto

Mechanical Engineering Department, NERIST, Arunachal Pradesh. E-mail: smh@nerist.ac.in

Wang and Russel [8] proposed minimax design method to construct the optimum shape under a finite range of tip loads and observed an increase of 643% in fundamental frequency. Xu and Ananthasuresh [9] employed sequential quadratic programming (SQP) method available in MATLAB for shape optimization of segment of compliant mechanism. Proposed objective function with a number of constraints tries to achieve the optimum balance between a flexibility measure and a stiffness measure. Examples indicate substantial improvement due to shape optimization.

Gunjal and Dixit [10] addressed the shape optimization of a rotating beam at different speeds with constraints on its mass and static tip deflection. They studied natural frequencies and dynamic response of the optimized beam. Dixit *et al.* [11] presented FEM model of single link flexible robotic manipulator for revolute and prismatic joint. They used SQP for optimizing beam shapes under different optimization conditions and compared its dynamic responses and fundamental frequencies.

In this work, author presented the optimized shapes for different payload cases which give the minimum of maximum dynamic tip deflection for that particular payload. Author also presented the dynamic response due to sinusoidal torque profile along with bang-2 torque and also the behaviour of the optimized manipulator for payloads other than the payload for which it is optimized.

2 Modelling and Solution Technique

High speed rotating flexible beams have significant transverse deflections. They behave as a nonlinear elastic beams and exhibit vibratory motions in both chord wise and flap wise directions. However, Robotic manipulators usually work at moderate peak speed. Induced transverse force in the chord wise direction due to the applied excitation torque is much higher compared to the gravity force in flap wise direction and vibrations are predominantly in chord wise directions. Formulations are consistently linearized for small transverse deflection due to bending motion under linear beam theory as a two-dimensional idealization. This simplified model is not suitable for modelling the dynamic behaviour of single link flexible manipulator with large deflections.

The finite element formulation has been described in Dixit *et al.* [11]. It is described here for the sake of completeness. Figure 1(a) shows single link flexible manipulator in which XOY and ROS represents the stationary and moving co-ordinate frames respectively. T represents the applied torque at the hub, q represents the loading intensity (load per unit length) in the transverse plane and E, I, L, ρ, A, J_h and M_p represents the Young's modulus, area moment of inertia, length, mass density, cross-sectional area, hub-inertia and payload of the manipulator respectively. Motion of the manipulator is represented by fixed XOY co-ordinate frame. Manipulator is considered slender. So, transverse shear and rotary inertia effects are neglected allowing it to be treated as an Euler-Bernoulli beam. Beam is assumed to vibrate dominantly in horizontal plane (XOY), neglecting gravity effects (acting in flap wise direction).

Consider an infinitesimal link element P on the manipulator at a distance 'x' from the hub. Position of the element P with respect to inertial frame of reference (XOY) after having rigid body motion $\theta(t)$ (rotation of moving frame ROS and trans

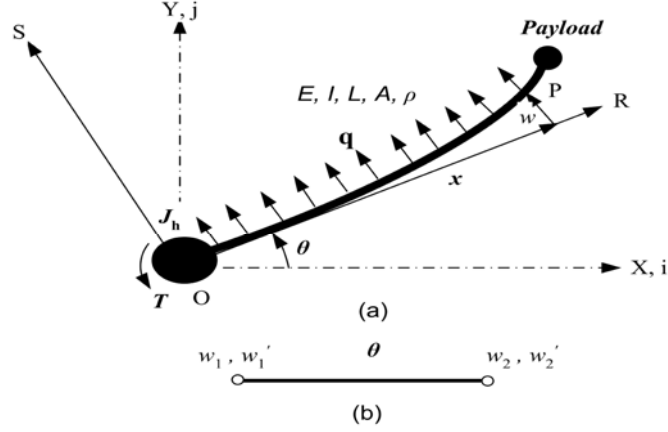


Figure 1. (a) Configuration of flexible manipulator, (b) typical finite element with five dof

-verse deflection $w(x, t)$ is given by the position vector $\mathbf{P}(x, w)$ with respect to the fixed frame

$$\mathbf{r}_P = \overrightarrow{OP} = (x \cos \theta - w \sin \theta) \hat{i} + (x \sin \theta + w \cos \theta) \hat{j} \tag{1}$$

and its square of the velocity can be expressed as

$$V_P^2 = \left| \dot{\mathbf{r}}_P \right|^2 = \dot{\theta}^2 \{x^2 + w^2\} + \dot{w}^2 + 2\dot{\theta}\dot{w}x. \tag{2}$$

By approximating $x^2 + w^2 \cong x^2$ for small transverse deflection ($x \gg w$), magnitude of velocity of the element P (V_P) can be obtained from Equation 1 as

$$V_P^2 = \left| \dot{\mathbf{r}}_P \right|^2 = x^2 \left(\frac{d\theta}{dt} \right)^2 + \left(\frac{\partial w}{\partial t} \right)^2 + 2x \frac{d\theta}{dt} \frac{\partial w}{\partial t}. \tag{3}$$

Kinetic energy (K), Potential Energy (U) and Work done on the system (W) are given by

$$K = \frac{1}{2} J_h \left(\frac{d\theta}{dt} \right)^2 + \frac{1}{2} \int_0^L m V_P^2 dx \tag{4a}$$

$$U = \frac{1}{2} \int_0^L EI \left(\frac{\partial^2 w}{\partial x^2} \right)^2 dx \tag{4b}$$

$$W = \frac{1}{2} \int_0^L q w dx + T \theta \quad (4c)$$

Using Extended Hamilton's principle, variational form for the equation of motion of the dynamic system is given by

$$\delta \int_{t_1}^{t_2} (K - U + W) dt = 0, \quad (5)$$

this gives

$$\frac{\partial^2}{\partial x^2} \left(EI \frac{\partial^2 w}{\partial x^2} \right) + m \frac{\partial^2 w}{\partial t^2} + mx \frac{d^2 \theta}{dt^2} - q = f_1 = 0 \quad (6)$$

and

$$J_h \frac{d^2 \theta}{dt^2} + \int_0^L mx \left(\frac{\partial^2 w}{\partial t^2} + x \frac{d^2 \theta}{dt^2} \right) dx - T = f_2 = 0, \quad (7)$$

where m (mass per unit length) and I are function of x and transverse load is the function of both x and t . The following geometry boundary conditions act at the torque end side:

$$w(0, t) = 0 \quad \& \quad \left. \frac{\partial w}{\partial x} \right|_{x=0} = 0. \quad (8)$$

The following natural boundary conditions act at the free end:

$$\left. \frac{\partial^2 w}{\partial x^2} \right|_L = 0 \quad \& \quad \left. \frac{\partial}{\partial x} \left(EI \frac{\partial^2 w}{\partial x^2} \right) \right|_L = 0. \quad (9)$$

In the FEM formulation the manipulator is divided into 20 elements, each element having five degrees of freedom as shown in Figure 1(b). In the figure, θ is the hub rotation and w_1, w_1', w_2, w_2' are the transverse deflection and slopes at the first and second nodes of the element. Using Galerkin's FEM approach with W as the weight function and v as the vertical deflection, weak form of the differential equation for an element is given by (from Equation 6)

$$\int_0^h W f_1(v) = 0$$

$$W \frac{\partial}{\partial x} \left(EI \frac{\partial^2 v}{\partial x^2} \right) \Big|_0^h - \frac{\partial W}{\partial x} \left(EI \frac{\partial^2 v}{\partial x^2} \right) \Big|_0^h + \int_0^h \frac{\partial^2 W}{\partial x^2} \left(EI \frac{\partial^2 v}{\partial x^2} \right) dx + \int_0^h m W \frac{\partial^2 v}{\partial t^2} dx - \int_0^h W q dx = 0. \quad (10)$$

Approximate vertical deflection including rigid body motion (θ) is expressed in matrix form

$$v = \begin{bmatrix} x & N_1 & N_2 & N_3 & N_4 \end{bmatrix} \begin{bmatrix} \theta \\ w_1 \\ w'_1 \\ w_2 \\ w'_2 \end{bmatrix} \quad (11)$$

where x is the local coordinate, h the element length and N_1, N_2, N_3 and N_4 are known as the Hermitian shape functions and Galerkin's weight function (W) is approximated in same fashion as v .

Effect of hub mass and payload mass is incorporated in the global mass matrix and stiffness matrix using Dirac-delta function as described by Dixit *et al.* [11]. Hub mass and tip mass/payload is defined in terms of β (ratio of hub mass to beam mass) and μ (ratio of payload to beam mass). Equation 10 can be expressed in matrix form:

$$\left[M^e \right] \{ \ddot{u} \} + \left[K^e \right] \{ u \} = \{ F^e \}. \quad (12)$$

Element system damping is employed using Rayleigh damping giving element damping matrix

$$\left[C^e \right] = \alpha \left[M^e \right] + \lambda \left[K^e \right], \quad (13)$$

where $\left[M^e \right]$, $\left[K^e \right]$ and $\{ F^e \}$ are the element mass matrix, stiffness matrix and element load vector and α and λ are the constants determined from different modal damping ratios. After assembling element equations, the global system governing equation can be expressed as

$$\left[M \right] \{ \ddot{X} \} + \left[C \right] \{ \dot{X} \} + \left[K \right] \{ X \} = \{ F \}, \quad (14)$$

where $\left[M \right]$, $\left[C \right]$ and $\left[K \right]$ are the global mass, damping and stiffness matrices respectively. Global load vector $\{ F \}$ and global nodal displacement vector $\{ X \}$ are given by

$$\{ F \} = \left[T \ 0 \ 0 \ \dots \ 0 \right]^T \text{ and } \{ X \} = \left[\theta \ w_1 \ w'_1 \ \dots \ w_N \ w'_N \right]^T. \quad (15)$$

Neglecting damping matrix and load vector, Equation 14 becomes standard eigenvalue problem, which is solved to obtain natural frequencies of the system. The Newmark integration scheme is basically the extension of the linear acceleration method. It is a constant average acceleration scheme. Using Newmark's method, transverse deflection w , rigid body motion θ and its derivative $\dot{\theta}$ are obtained.

3 Optimization Procedure

Minimization of maximum dynamic tip deflection is considered as an objective for high speed operation of the robotic system. Minimization of static deflection as well as mass of the uniform beam manipulator is kept constraints. General form of an optimization problem is expressed as

$$\begin{aligned} & \text{Minimize } f(X), \\ & \text{subject to} \end{aligned} \quad (16a)$$

$$M - M^* \leq 0 \quad (16b)$$

$$\delta - \delta^* \leq 0 \tag{16c}$$

and

$$X^L \leq X \leq X^U \tag{16d}$$

where $X = [d_1 \ d_2 \ \dots \ d_{20}]^T$ is a design vector with d_i indicating diameter of the i^{th} finite element, $f(X)$ indicates the objective function (maximum dynamic tip deflection of single link flexible manipulator). X^L and X^U are the vectors of lower and upper bounds of design variables respectively. M is the mass of the optimized manipulator, M^* is the prescribed mass of the uniform beam manipulator and δ_{tip} , δ_{tip}^* are the static tip deflection of the optimized manipulator and uniform beam manipulator respectively. The MATLAB function “*fmincon*” uses SQP for constrained optimization of nonlinear function.

4 Results and Discussion

A comparative dynamic analysis has been carried out for shape optimized single link revolute flexible manipulator. For the numerical study, a manipulator having uniform diameter 10 mm, length 750 mm, mass 159.6 gm, Young’s modulus of elasticity 71 GPa is considered. Its modal damping ratios for the first and second mode are taken as 0.011 and 0.029 respectively based on Dixit *et al.* [11]. Optimized beams are subjected to a bang-bang torque of magnitude 0.5 N-m (Figure 2) about the axis of rotation.

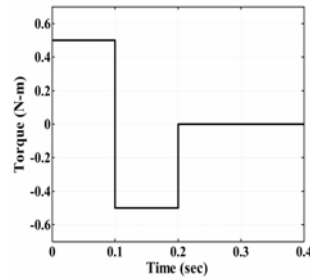


Figure 2: Bang-2 torque

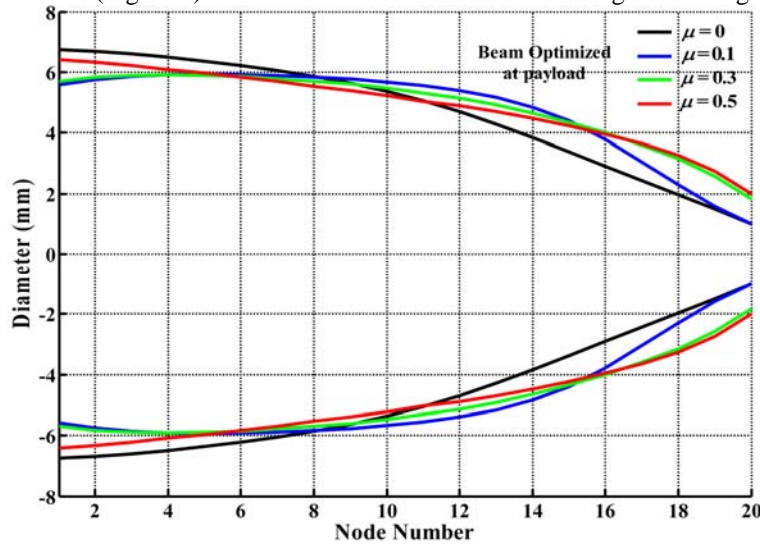


Figure 3: Optimized shapes for different payloads (μ)

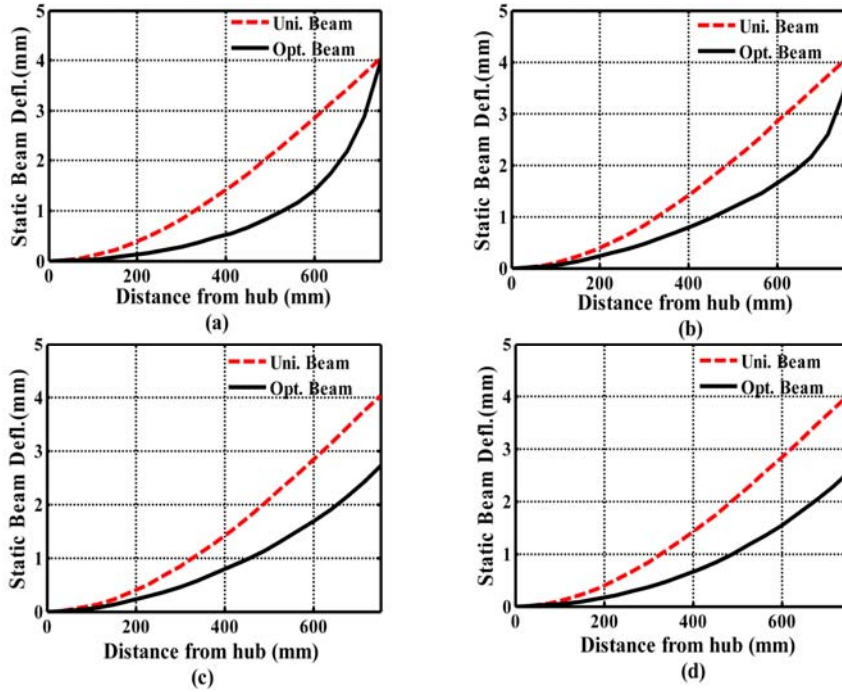


Figure 4: Comparison of static beam deflection, beam optimized at (a) $\mu=0$, (b) $\mu=0.1$, (c) $\mu=0.3$ & (d) $\mu=0.5$

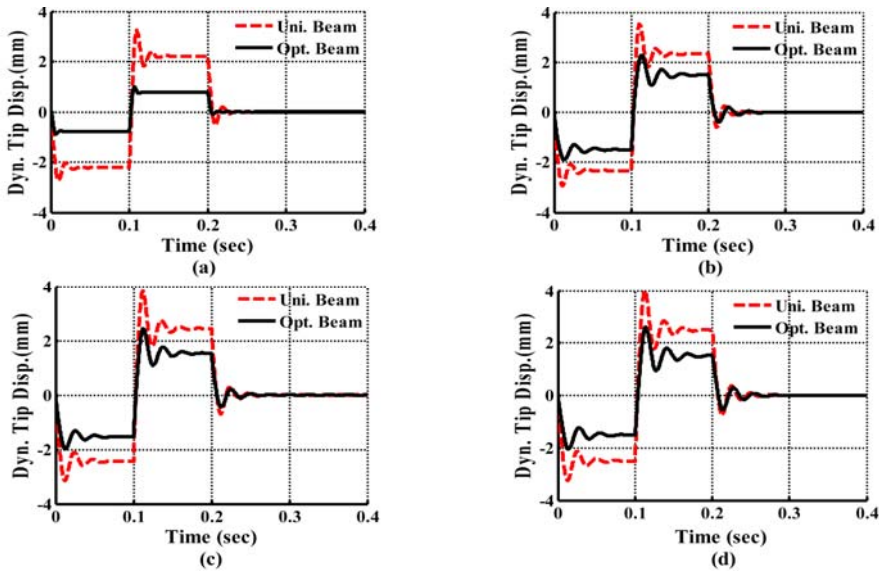


Figure 5 : Comparison of dynamic tip deflection due to bang-2 input torque, beam optimized at (a) $\mu=0$, (b) $\mu=0.1$, (c) $\mu=0.3$ & (d) $\mu=0.5$

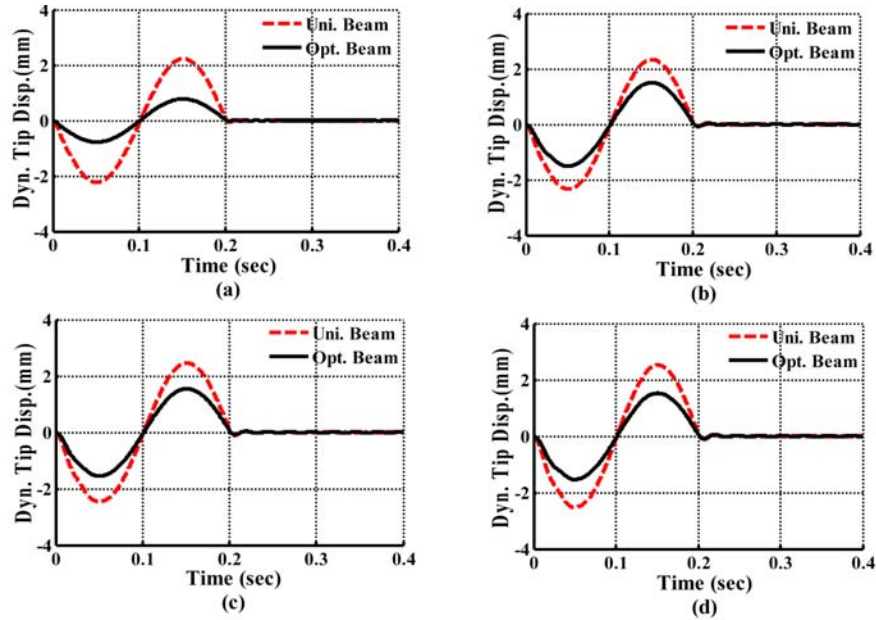


Figure 6: Comparison of dynamic tip deflection due to sinusoidal input torque, beam optimized at (a) $\mu=0$, (b) $\mu=0.1$, (c) $\mu=0.3$ & (d) $\mu=0.5$ (with corresponding payload)

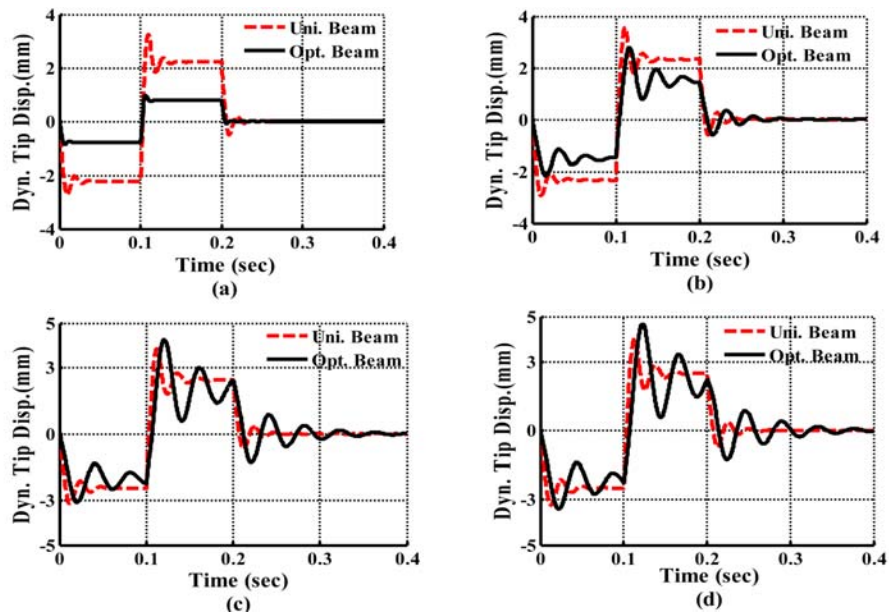


Figure 7: Comparison of dynamic tip deflection due to bang-2 input torque, beam optimized at $\mu=0$ with payload (a) $\mu=0$, (b) $\mu=0.1$, (c) $\mu=0.3$ & (d) $\mu=0.5$

For comparative static tip deflections, 1 N static load is considered at the end of the manipulator. Optimized shapes of the manipulator as per the optimization problem defined in Equation 16 are plotted in Figure 3. There are different optimal shapes for different payloads. These shapes give minimum of the maximum dynamic tip deflection. Static tip deflections due to applied 1N force at the tip are shown in Figure 4. Optimized beams deflect less than the static tip deflection of the uniform beam manipulator which well satisfies the constraint imposed in the optimization problem definition. Dynamic tip deflection due to bang-2 torque is shown in the Figure 5. All optimized beams have minimum tip deflection than the uniform beam manipulator for the corresponding payload for which it is optimized. Dynamic tip deflections are also plotted for sinusoidal torque ($T = 0.5 \sin 10\pi t$, $0 \leq \text{time}(t) \leq 0.2$, else $T = 0$) in Figure 6. It is observed same trends of behaviour of the optimized beams under different excitations. Dynamic tip deflections of the beam optimized for no payload ($\mu=0$) as shown in Figure 7. It doesn't give minimum tip deflection than uniform beam manipulator for higher payload cases. However, beam optimized for higher payload always gives minimum of maximum dynamic tip deflection with respect to that of uniform beam manipulator for range of payloads with little higher maximum dynamic tip deflection at lower payloads.

5 Conclusion

In this work, the problem of minimization of maximum dynamic tip deflection is carried out through linear modeling of single link flexible revolute manipulator. Thorough FE analysis has been conducted and successive SQP iteration scheme has been used to solve constrained optimum shape of the flexible manipulator to minimize the maximum dynamic tip deflection.

There are different optimal shapes for different payloads. These optimum shapes give minimum of the maximum dynamic tip deflection for that particular payload. Beam optimized for higher payload always gives minimum of maximum dynamic tip deflection with respect to that of uniform beam manipulator for range of payloads but not the beam optimized for no payload ($\mu=0$) case.

References

- [1] E.T. Cranch and A.A. Adler, "Bending vibration of variable cross-section beams", *J. of Applied Mechanics*, ASME, vol.23(1), pp.103-108, 1956.
- [2] A.C. Heidebrecht, "Vibration of non-uniform simply supported beams", *J. of Engineering Mechanics Division*, proceeding of the ASCE, vol. 93(EM2), pp. 1-15, 1967.
- [3] C.D. Bailey, "Direct analytical solution to non-uniform beam problem", *J. of Sound and Vibration*, vol. 56(4), pp. 501-507, 1978.
- [4] B.L. Karihaloo and F.I. Niordson, "Optimum design of vibrating cantilever", *Journal of Optimization, Theory and Applications*, vol. 11(6), pp. 638-654, 1973.

- [5] Y.S. Lio, “A generalized method for the Optimal Design of Beams under Flexural Vibration”, *Journal of Sound and Vibration*, vol. 167(2), pp. 193–202, 1993.
- [6] Fei-Yue Wang, “On the External Fundamental Frequencies of one Link Flexible Manipulators”, *The International Journal of Robotics Research*, vol. 13, pp. 162–170, 1994.
- [7] F.Y. Wang and L. Meirovitch, “Optimum Design of Vibrating Cantilevers: A classical problem. Revisited”, *Journal of Optimization Theory and Applications*, vol. 84(3), pp. 635–652, 1995.
- [8] F.Y. Wang, and J.L. Russel, “Optimum Shape Construction of Flexible Manipulators with Total Weight Constraint”, *Systems, Man and Cybernetics*, vol. 25(4), pp. 605–614, 1995.
- [9] D. Xu, and G.K. Ananthasuresh, “Freeform Skeletal Shape Optimization of Compliant Mechanism”, *Journal of Mechanical Design*, vol. 125, pp. 253–261, 2003.
- [10] S.K. Gunjal, and U.S. Dixit, “Vibration Analysis of Shape Optimized Rotating Cantilever Beam”, *Engineering Optimization*, vol. 39(1), pp. 105–123, 2007.
- [11] U.S. Dixit, R. Kumar and S.K. Dwivedy, “Shape Optimization of Flexible Robotic Manipulator”, *ASME Journal of Mechanical Design*, vol. 121(3), pp. 559–565, 2006.